Aspects of the Mechanism of Catalysis in Phospholipase A_2. A Combined *ab initio* Molecular Orbital and Molecular Mechanics Study

Bohdan Waszkowycz and Ian H. Hillier *
Chemistry Department, University of Manchester, Manchester M13 9PL
Nigel Gensmantel and David W. Payling
Fisons p.l.c., Pharmaceutical Division, Bakewell Road, Loughborough, Leicestershire, LE11 0RH

A combination of *ab initio* molecular orbital and molecular mechanics calculations has been used to estimate the energetics of the formation of the tetrahedral intermediate involved in the catalytic ester hydrolysis by the enzyme PLA2. A number of models have been studied which differ in the extent to which the environment of the enzyme is included. The calculations provide support for the mechanism of catalysis involving nucleophilic attack of water activated by proton transfer to His-48. A single, rather than a double, proton-transfer mechanism, involving His-48, is favoured.

Phospholipase A_2 (PLA2) is a ubiquitous enzyme which hydrolyses phospholipids, the components of cell membranes, to release fatty acids such as arachidonic acid, thus initiating the production of a wide range of cellular mediators such as the prostaglandins.[1] An understanding of the mechanism of the catalysis by PLA2 is of practical importance in view of the current search for medically useful inhibitors of the enzyme.

Such a mechanism has been proposed by Verheij *et al.*[2] based on the *X*-ray crystal structure of PLA2,[3] which shows similarities to that of other hydrolytic enzymes such as the serine proteases. However, this mechanism has yet to be proven experimentally so that theoretical investigations of the various aspects of it are potentially useful.

In this paper we study this mechanism by means of *ab initio* molecular orbital (MO) calculations on models of a substrate [1,2-dilauroyl-DL-phosphatidyl ethanolamine, (**1**)] within the active site of the enzyme and determine the role of the local environment of the active site on the energetics of the hydrolysis reaction.

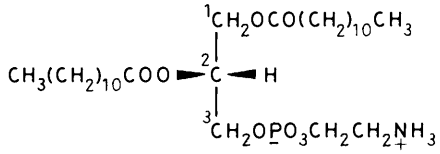

(**1**)

In any model of enzyme catalysis some form of molecular orbital calculation is essential to quantify the energies involved in the breaking and formation of bonds, and such techniques have been applied to a number of enzymes to various degrees of sophistication. All realistic MO calculations are severely limited as to the number of atoms which can be included in the model, and hence several studies have simplified the complex environment of the active site by modelling a small number of molecules *in vacuo*.[4–6] However, in general an active site can be represented accurately only by the inclusion of a substantial number of residues positioned according to the known enzyme structure. For such a model, the number of atomic basis functions needed for a MO calculation will usually exceed the available computational resources. However, it is possible to represent much of the active site solely as point charges (integral or partial), which are incorporated into the one-electron Hamiltonian, and which simulate the electrostatic influence of the environment on the electronic wavefunction of the reacting system. The importance of this effect in the activation of a substrate or stabilisation of a transition state has been demonstrated in studies of carboxypeptidase,[7–9] papain,[10] and trypsin.[11,12]

A purely quantum mechanical model cannot, due to computational restrictions, allow for the optimisation of the changing conformational environment of the active site during the catalytic reaction. This can, however, be achieved by the use of molecular mechanics, with which structures of minimum conformational/steric energy can be found readily for systems as large as proteins. Such minimisations are valuable in the refinement of *X*-ray crystal structures and for the modelling of enzyme-substrate complexes.[13,14] The techniques of molecular mechanics and quantum mechanics are thus complementary, as demonstrated by recent work on catalysis in lysozyme,[15] papain,[16] triosephosphate isomerase,[17] and trypsin.[18]

In the work presented herein we adopt the strategy of using computer graphics and molecular mechanics minimisations to model the initial PLA2-substrate complex, for which no crystal structure is available, in order to obtain intermolecular geometries to be used in subsequent *ab initio* MO calculations. In these latter calculations up to 24 atoms have been treated explicitly to represent the substrate and the catalytically important residues. A further 27 atoms in the immediate environment have been incorporated into the model solely as point charges.

The proposed mechanism[2] of catalysis can be briefly described. The *X*-ray crystal structure of PLA2 reveals a hydrogen-bonded histidine-aspartate couple in the active site (His-48 and Asp-99 of bovine pancreatic PLA2), which is a feature common to other hydrolytic enzymes such as the serine-histidine-aspartate charge relay triad of the serine proteases. In PLA2 there is no serine available locally, so that it is probable that a water molecule in the active site becomes the active nucleophile upon proton transfer to histidine (Figure 1). The attack by water on the C-2 carbonyl of the phospholipid leads to the formation of a tetrahedral oxyanion intermediate, which is stabilised electrostatically by a calcium ion and by hydrogen-bonding to the backbone –NH of Gly-30. The oxyanion breaks down, on proton transfer from His-48, to release the C-2 fatty acid. In the original description of the charge relay triad[19] it was suggested that the system was stabilised by a concerted second proton transfer from N-ε2 of histidine to aspartate, such that the histidine cation-aspartate anion couple becomes a neutral histidine-aspartic acid couple. However, recent experimental[20] and computational[6,11,12] work suggest that the second proton

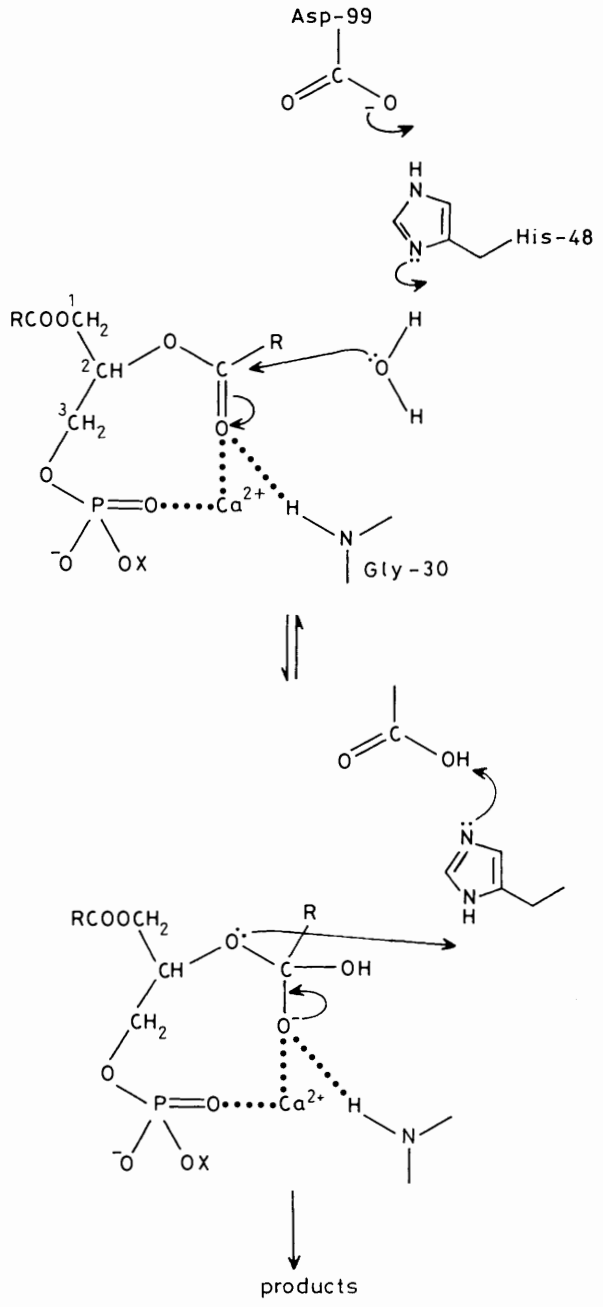

Figure 1. Proposed mechanism of catalysis in PLA2.

transfer does not occur in the serine proteases, since the ionic couple is more stable in the environment of the active site than is the neutral couple. By analogy, it is possible that only a single proton transfer occurs in PLA2.

We present herein preliminary calculations on the potential energy surface for catalysis by PLA2, and investigate the influence of the active site on the energetics of formation of the oxyanion intermediate. The energetics of the single and double proton transfer mechanisms are also studied, since they emphasise the dependence of the model on the choice of basis set and on the adequate simulation of the local environment.

Computational Details.—The molecular mechanics facility within the program AMBER,[21] together with the computer graphics model building facility within the Chem-X system[22] were used to build and energy-minimise models of a phospholipid substrate (1,2-dilauroyl-DL-phosphatidylethanolamine, I)[23] within the active site of PLA2. The calculations were facilitated by use of an interface between AMBER and Chem-X written by us. The structure of PLA2 was taken from the *X*-ray crystal co-ordinates of bovine pancreatic PLA2.[3] The phospholipid fits into the active site with minimal distortion of dihedral angles. The C-2 carbonyl and the C-3 phosphate become ligands of the calcium ion, so that the carbonyl group is found to be tightly held in a position adjacent to the attacking water molecule, already present in the crystal structure, and His-48. The substrate's long parallel acyl chains extend from the active site into the solvent.

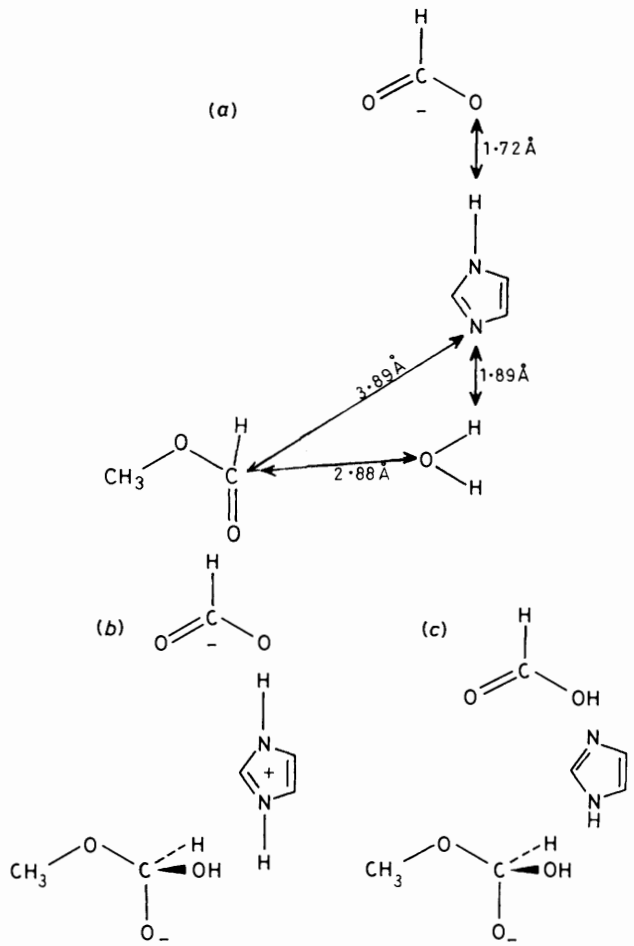

Figure 2. Supermolecule models treated explicitly in M.O. calculations: (*a*) reactants; (*b*) intermediates (single proton transfer); and (*c*) intermediates (double proton transfer).

The final model used consisted of a complete PLA2 molecule (123 amino acids, with each C–H group treated as a united atom), the phospholipid substrate and solvent (106 water molecules from the *X*-ray structure, plus a further 640 water molecules added by AMBER to fully solvate the system). In all, this model contained close to 3 500 atoms, and was energy minimised to provide intermolecular geometries which were used in the subsequent MO calculations. The structure of the minimised enzyme-substrate system is shown in Plate 1.

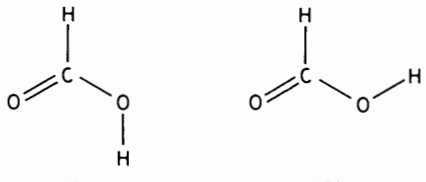

(2) (3)

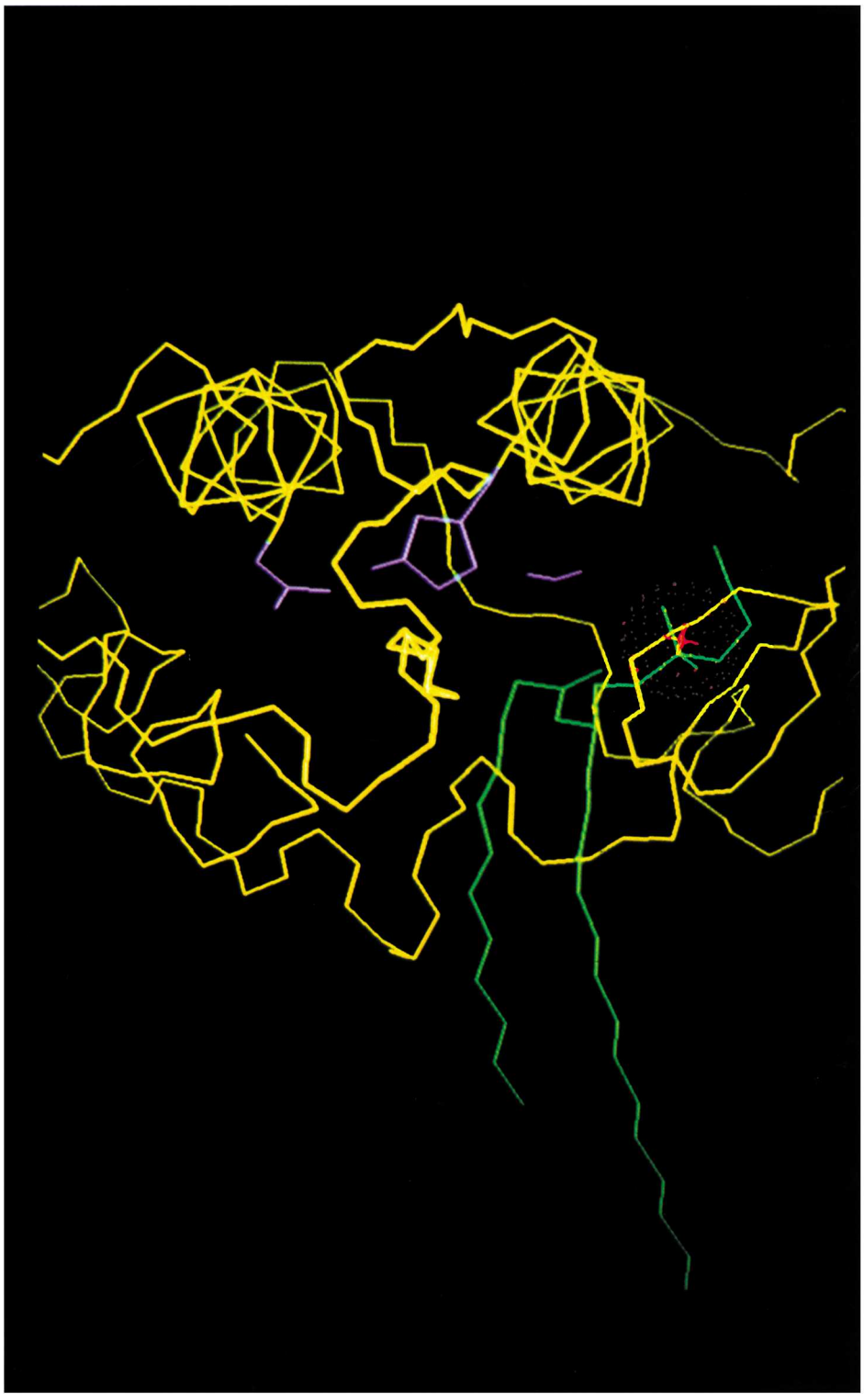

Plate 1. The structure of the PLA2-substrate model after AMBER minimisation. For clarity the enzyme is shown as the peptide backbone (yellow, with the calcium ion represented by a red dot surface) and with water omitted. The phospholipid substrate (green, hydrogens omitted) is bound to the calcium ion such that the C-2 carbonyl is adjacent to the attacking water molecule and to the side-chains of His-48 and Asp-99 (all highlighted in purple).

[*To face* p. 1796

Plate 2. The active site residues which were modelled in the MO calculations, as they appear in the PLA2-substrate model after AMBER minimisation. The calcium ion (yellow dot surface) binds the C-2 carbonyl and the phosphate of the substrate (depicted as a small fragment for clarity) as well as the backbone carbonyls of Tyr-28, Gly- 30, and Gly-32, and the carboxylate of Asp-49 (all oxygens highlighted in red). The imidazole ring of His-48 is proposed to be hydrogen-bonded to two water molecules (the water labelled 2 is the active nucleophile) and to the carboxylate of Asp-99; the latter is also hydrogen-bonded to two further water molecules and to the phenolic hydroxyls of Tyr-52 and Tyr-73.

The MO calculations were carried out for two points on the potential energy surface of the hydrolysis reaction in order to characterise the size of the energy difference between the reactants and the oxyanion intermediate. The following systems were used to model the actual reaction. The first [Figure 2(*a*)] was a model of the reactants only, as positioned in the active site. Here methyl formate models the substrate, imidazole models His-48, and the formate anion models Asp-99. The second system represents the formation of the oxyanion intermediate by both the single and the double proton transfer mechanisms [Figures 2(*b*) and 2(*c*), respectively]. The formic acid in Figure 2(*c*) was modelled in the two conformations, (**2**) and (**3**).

The geometries of the various molecules in Figure 2 were obtained by optimising each species using an STO-3G basis. Full geometry optimisation was performed using analytic gradient methods as implemented in the program GAMESS.[24] We assume that the oxyanion is not a transition state, but an intermediate which occupies a minimum on the potential energy surface. (According to the proposed mechanism, two transition states will be involved, one leading to the formation of the intermediate and one leading to its breakdown). Such tetrahedral intermediates have been isolated for other hydrolytic enzymes,[20] and are generally assumed to be similar to the transition state in structure and energy.[11,12] For our purposes, we are proposing that the effect of the active site residues in reducing the potential energy barrier of the overall reaction can be estimated by observing their effect on the energy of the intermediate.

The optimal molecular geometries were then used, in conjunction with intermolecular geometries obtained from molecular mechanics energy minimisations of PLA2, to build a series of supermolecule models of the reaction. Single-point energy calculations were performed on these supermolecules using both STO-3G and 4-31G basis sets. The intermolecular geometries used for the model of the reactants were kept constant, as far as possible, for the model of the intermediates. Although this assumes that there are no conformational changes to the active site on formation of the oxyanion, it allows a direct comparison to be made of the energies of each model, which might otherwise be obscured by perhaps significant changes in intermolecular geometry.

The supermolecule models that we have examined are summarised in Table 1. Model 1 represents the ester plus water plus imidazole forming the oxyanion plus imidazolium. In Model 2 the role of the formate anion is considered, together with the relative preference for the single or double proton transfer mechanisms [Models (2*a*) and 2(*b*), respectively]. In further models, additional regions of the active site are represented by point partial charges. These are based on the AMBER database charges, though simplified, and are positioned according to the nuclear co-ordinates of polar functional groups in close proximity to the catalytically important residues. Model 3 includes the calcium ion as a +2 point charge. This is an unrealistic simulation of calcium in its immediate environment and thus Model 4 includes the following ligands of calcium: three carbonyl groups (Tyr-28, Gly-30, Gly-32), each simplified to point charges of +0.5 (carbon) and −0.5 (oxygen); a carboxylate, Asp-49 (+0.5 [carbon]) and 2 × −0.75 [oxygen]); a single phosphoryl oxygen (+0.5 [phosphorus] and −0.5 [oxygen]) (Figure 3). Model 5 includes the environment of Asp-99, in order to assess whether the relative stabilities of formate and formic acid are influenced by their hydrogen-bonded environments. Within hydrogen-bonding distance of the carboxylate of Asp-99 are two phenolic hydroxyls (Tyr-52 and Tyr-73, represented by charges of +0.3 [hydrogen] and −0.3 [oxygen]) and two water molecules (+0.3 [hydrogens], −0.6 [oxygens]) (Figure 4). There is a bad steric contact between the acidic proton of formic acid in conformation (**2**) and

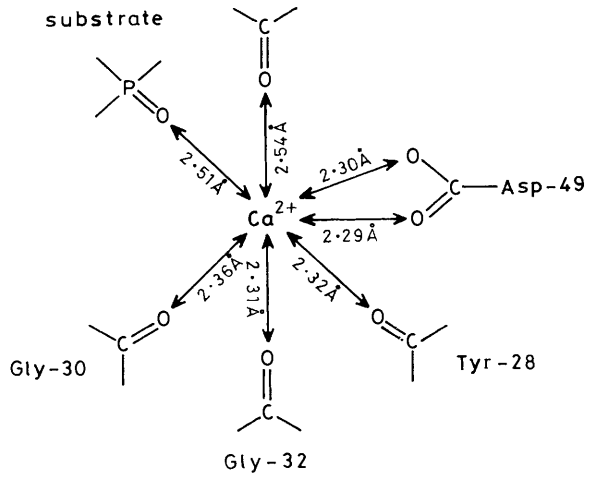

Figure 3. Ligands of Ca^{2+} ion.

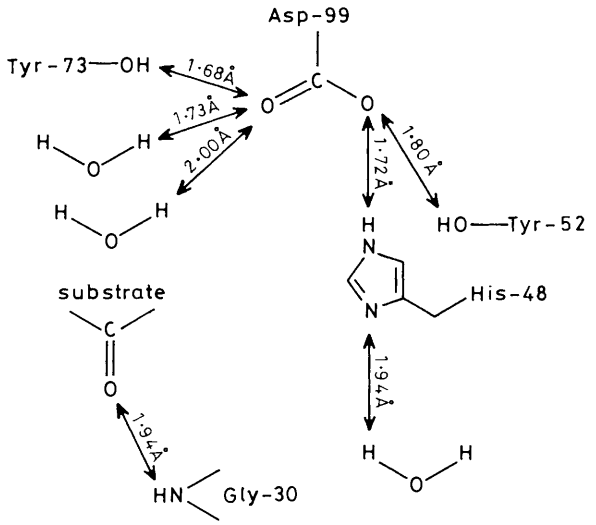

Figure 4. Hydrogen-bonded environment of His-48, Asp-99, and the substrate C-2 carbonyl.

the hydroxyl hydrogen of Tyr-52, but no bad contact for formate or formic acid in conformation (**3**). Formic acid (**2**) was used in previous models because it is appreciably more stable than (**3**) due to intramolecular hydrogen-bonding. In Model 5 both conformations are evaluated [Models 5(*b*) and 5(*c*)] and in one further calculation [Model 5(*d*)] the environment is modified to accommodate formic acid in conformation (**2**), by rotation of the hydroxyl of Tyr-52 through 180° to relieve the bad contact. The final calculation, Model 6, incorporates the –NH group of Gly-30 (point charges of +0.3 [hydrogen], −0.3 [nitrogen]), which, with calcium, stabilises the negative charge of the oxyanion. The model also includes a further water molecule which lies in the active site, hydrogen-bonded to N-1 of His-48. This water molecule hinders the formation of the oxyanion and was therefore repositioned by means of a molecular mechanics minimisation within a fixed model of the active site.

All calculations were carried out on the FPS M64/60 of the Computational Chemistry Group of Manchester University.

Computational Results and Discussion.—Figures 2–4 present relevant intermolecular distances in order to give some indication of the geometry of the models used in the MO calculations (full Cartesian co-ordinates are available on request to B.W.). Plate 2 shows the spatial arrangement of these residues in the active site. Total energies for the reactants are

Table 1. Supermolecular models used in single point MO calculations.

Model					
1	2	3	4	5	6
Ester + imidazole + HOH ⟶ oxyanion + imidazolium	Ester + imidazole + HOH + $HCOO^-$ ⟶ (*a*) oxyanion + imidazolium + $HCOO^-$ (*b*) oxyanion + imidazole + HCOOH (**2**)	(*a*), (*b*): as for 2(*a*) and 2(*b*), with Ca^{2+} as point charge	(*a*), (*b*): as for 3(*a*) and 3(*b*), with calcium ligands as point charges. (*c*): as for 4(*b*) with HCOOH (**3**)	(*a*), (*b*), (*c*): as for 4(*a*), (*b*), and (*c*), with environment of Asp-99 (point charges) (*d*): as for 5(*b*), *i.e.* HCOOH (**3**), but with repositioned point charges	(*a*), (*b*): as for 5(*a*) and (*c*), *i.e.* HCOOH (**3**), with environment of substrate and His-48 (as point charges)

Table 2. Total energies (a.u.) for models of reactants.

Model	STO-3G	4-31G
1	−521.758 583	−527.819 956
2	−707.275 038	−715.770 429
3	−707.466 657	−716.010 799
4	−708.624 418	−717.144 251
5	—	−717.635 448
6	—	−717.878 196

Table 3. Energy difference (ΔE) to the formation of intermediates (kcal mol^{-1}).

Model[a]	STO-3G	4-31G
1	+95.1	+52.0
2(*a*) (SPT)	+65.3	+30.9
2(*b*) (DPT) (**2**)	+9.8	+47.2
3(*a*) (SPT)	+3.1	−15.6
3(*b*) (DPT) (**2**)	−74.1	−19.5
4(*a*) (SPT)	+20.6	−3.1
4(*b*) (DPT) (**2**)	−42.0	+6.3
4(*c*) (DPT) (**3**)	−37.8	+13.7
5(*a*) (SPT)		+9.5
5(*b*) (DPT) (**2**)		+49.2
5(*c*) (DPT) (**3**)		+31.1
5(*d*) (DPT) (**2**)*		+28.6
6(*a*) (SPT)		+9.7
6(*b*) (DPT) (**3**)		+33.2

[a] SPT, DPT—single, double proton transfers; (**2**), (**3**)—conformations of HCOOH; *—modified environment.

given in Table 2 and the calculated value of ΔE for each model is given in Table 3. Here ΔE is the difference between the total energy of the reactants and of the tetrahedral intermediate. A positive value of ΔE represents an endothermic reaction. The STO-3G values are quoted for the first four models to emphasise the discrepancy between the minimal and extended basis set energetics. In particular, with the STO-3G basis set the value of ΔE for double proton transfer is much lower than that for single proton transfer (by up to 77 kcal mol^{-1}, for Model 3), whereas with the 4-31G basis set the two systems are of comparable stability, with the single proton transfer being favoured overall. This deficiency of minimal basis sets is well known. Thus, early computational studies on the charge relay triad in the serine proteases favoured the double proton transfer mechanism,[25–27] because their use of minimal basis sets and semi-empirical methods led to inaccuracies in the evaluation of proton affinities, whereas more recent calculations have stressed

Table 4. 4-31G Mulliken populations for the carbonyl group of the reactant ester (R) and the oxyanion intermediate (**1**) (single proton-transfer mechanism).

	Model	Carbon	Oxygen
1	R	+0.63	−0.56
	(**1**)	+0.71	−0.83
2	R	+0.63	−0.57
	(**1**)	+0.72	−0.84
3	R	+0.75	−0.89
	(**1**)	+0.76	−1.12
4	R	+0.70	−0.72
	(**1**)	+0.74	−0.96
5	R	+0.70	−0.72
	(**1**)	+0.74	−0.96
6	R	+0.71	−0.75
	(**1**)	+0.73	−0.99

the necessity of using larger basis sets to obtain meaningful energetics.[6,11,12] Therefore, the remainder of this discussion will focus on the results obtained using a 4-31G basis, which in general accurately reproduces experimental proton affinities.[6,26] Although it is preferable to employ as large and as diffuse a basis set as is practicable for the size of system, at this stage of our calculations the 4-31G basis set is adequate in determining an approximate potential energy surface for this large system. More diffuse basis sets or calculations including correlation effects can be incorporated at a later stage when the active site model has been refined further.

The value of ΔE for the formation of the oxyanion is initially large (+52 kcal mol^{-1} for Model 1). The addition of the formate anion stabilises the oxyanion–imidazolium couple by 21 kcal mol^{-1} for the single proton-transfer mechanism [Model 2(*a*)] but by only 5 kcal mol^{-1} for the double proton-transfer mechanism [Model 2(*b*)]. The simulation of the calcium ion as a bare +2 charge (Model 3) is clearly unrealistic and results in a large negative ΔE value, and also obscures the preferential stabilisation of the single *versus* the double proton-transfer mechanism. The value of ΔE has been reduced because while the calcium ion lowers the total energy of both the ester and the oxyanion, it has a greater electrostatic effect on the latter because of the greater electron density on the oxygen of the oxyanion (Table 4).

Model 4 includes the carbonyl and carboxylate groups of the residues which form the calcium-binding loop. Although the sum of the point charges is still +2, the formal charge on the calcium has been reduced (the inclusion of the point charges in effect increases the dielectric of the system) and ΔE is now −3.1 kcal mol^{-1} for single proton-transfer and +6.3 kcal mol^{-1} for double proton-transfer. ΔE for the formation of formic acid in conformation (**3**) (with no internal hydrogen-bonding) is also presented to emphasise that, in the absence of the local environment of Asp-99, the loss of intramolecular hydrogen-

bonding is not compensated by hydrogen-bonding to imidazole, and hence for Model 4(*c*) [with (**3**)], ΔE is 7.4 kcal mol^{-1} greater than for Model 4(*b*) [with (**2**)].

The relative stabilities of the single and double proton-transfer models are dependent on the immediate environment of the imidazole-formate couple. Thus, a polar environment would be expected to favour a charged couple (imidazolium-formate) rather than a neutral couple (imidazole-formic acid.[12,28] To investigate the effect of the environment, Model 5 includes the residues which are hydrogen-bonded to Asp-99. (Note that His-48 is hydrogen-bonded only to Asp-99, the attacking water molecule and one further water molecule, which is simulated in the final model.) The effective negative charge on the formate is now reduced leading to a reduction in the electrostatic interaction between formate and imidazolium. ΔE for the single proton-transfer is now increased by 12.6 kcal mol^{-1} and for the double proton transfer [formic acid (**3**)] by 17.4 kcal mol^{-1}, compared to Model 4. Hydrogen-bonding therefore favours formate over formic acid and hence further supports the single proton transfer mechanism. [The formation of formic acid in conformation (**2**) is sterically hindered by the hydroxyl of Tyr-52. If this hydroxyl is moved to relieve the bad contact *e.g.* Model 5(d), the energies for the formation of (**2**) and (**3**) become comparable]. Thus the role of formate in the catalytic mechanism is in the stabilisation of the imidazolium cation by an electrostatic interaction rather than by being the final proton acceptor in a charge relay system.[29]

ΔE is found to change little in the final Model 6. The additional stabilisation of the oxyanion by hydrogen-bonding to the –NH of Gly-30 is offset by the inclusion of a further water molecule, hydrogen-bonded to N-1 of imidazole, which will to a small degree destabilise the imidazolium-formate couple in a manner analogous to the addition of the environment around formate in the previous model.

The final value of ΔE for the formation of the oxyanion is therefore +9.7 kcal mol^{-1}, for single proton-transfer, which represents a significant decrease compared with the previous models. However, the final model needs to be further refined in several ways. The point charge model is over-simplified and should be extended to include more active site residues in the MO calculation. Secondly, we have used a static environment which assumes that the conformation of the active site is the same for both reactants and intermediates. Although this has enabled us to present a direct comparison of the energies of reactants and intermediates, it is clearly not the most realistic representation of the active site during catalysis. Thus, a full molecular mechanics minimisation of the active site should be carried out for the formation of the oxyanion, for both the single and double proton-transfer models, in order to account for the way in which the active site accommodates each species. However, it would seem unlikely that our calculated energies would be altered to any great extent. It is probably more important to obtain a better estimate of the structure of the oxyanion. Whereas we have modelled the tetrahedral intermediate formed by the addition of hydroxide to a small ester *in vacuo*, it is clearly preferable to attempt to model the intermediate obtained for a large phospholipid *in situ*, where the shape of the intermediate may be influenced by steric and electrostatic interactions with the active site. For PLA2 these interactions may be of particular importance since the phospholipid C-2 carbonyl is strongly polarised by the calcium ion, while the cramped interior of the active site may hinder the $sp^2 \longrightarrow sp^3$ rehybridization at the carbon. The structure of the intermediate may well differ significantly from the oxyanion modelled here, so that it is not considered worthwhile to develop too elaborate a model of the active site until this structure is known.

In a similar way, it may be possible to investigate the structures of the transition states involved during the reaction. This is a difficult task because of the size of the molecules involved and the need to use a large basis set in order to reproduce accurately relative proton affinities. There is also the problem that the transition states are likely to be particularly unstable in any *in vacuo* model, where they are not constrained in space and stabilised electrostatically by the active site.

Conclusions

We have presented some initial calculations of the potential energy surface for hydrolysis of an ester in a simple model of the active site of PLA2. Although this model will benefit from further refinement, the results provide some theoretical evidence in favour of the proposed mechanism of catalysis *via* nucleophilic attack by a water molecule (upon concerted proton transfer to His-48), in as much as they show quantitatively how an oxyanion intermediate can be stabilised by electrostatic interaction with the surrounding environment (most importantly with the calcium ion and the histidine-aspartate couple). In agreement with recent computational and experimental work on the charge relay triad, the single proton-transfer mechanism is favoured, particularly when the environment of the His-Asp couple is included in the model.

The accuracy of simulations of this type is clearly dependent both on the size of the system explicitly considered and on the level of the computational method employed. The calculations described herein show that for simulation of enzyme catalysis a combined molecular mechanics and quantum mechanics approach is preferable to either technique used alone, in that it can quantify enthalpies of bond breaking and formation, as well as describe macromolecular conformational changes.

Acknowledgements

We thank the S.E.R.C. for support of this research.

References

1 A. J. Slotboom, H. M. Verheij, and G. H. de Haas, *New Comprehensive Biochemistry*, 1982, **4**, 354.
2 H. M. Verheij, J. J. Volwerk, E. H. Jansen, W. C. Puyk, B. W. Dijkstra, J. Drenth, and G. H. de Haas, *Biochemistry*, 1980, **19**, 743.
3 B. W. Dijkstra, K. H. Kalk, W. G. J. Hol, and J. Drenth, *J. Mol. Biol.*, 1981, **147**, 97.
4 R. Broer, P. T. van Duijnen, and W. C. Nieuwpoort, *Chem. Phys. Lett.*, 1976, **42**, 525.
5 C. A. Deakyne and L. C. Allen, *J. Am. Chem. Soc.*, 1979, **101**, 3951.
6 P. A. Kollman and D. M. Hayes, *J. Am. Chem. Soc.*, 1981, **103**, 2955.
7 D. M. Hayes and P. A. Kollman, *J. Am. Chem. Soc.*, 1976, **98**, 7811.
8 L. C. Allen, *Ann. N.Y. Acad. Sci.*, 1981, **367**, 383.
9 S. Nakagawa and H. Umeyama, *J. Theor. Biol.*, 1982, **96**, 473.
10 P. T. van Duijnen, B. T. Thole, R. Broer, and W. C. Nieuwpoort, *Int. J. Quant. Chem.*, 1980, **17**, 651.
11 S. Nakagawa and H. Umeyama, *J. Mol. Biol.*, 1984, **179**, 103.
12 H. Umeyama, S. Hirono, and S. Nakagawa, *Proc. Natl. Acad. Sci. USA*, 1984, **81**, 6266.
13 J. M. Blaney, P. K. Weiner, A. Dearing, P. A. Kollman, E. C. Jorgensen, S. Oatley, J. Burridge, and C. C. F. Blake, *J. Am. Chem. Soc.*, 1982, **104**, 6424.
14 G. Wipff, A. Dearing, P.K. Weiner, J. M. Blaney, and P. A. Kollman, *J. Am. Chem. Soc.*, 1983, **105**, 997.
15 A. Warshel and M. Levitt, *J. Mol. Biol.*, 1976, **103**, 227.
16 G. Bolis, M. Ragazzi, D. Salvaderi, D. R. Ferro, and E. Clementi, *Gazz. Chim. Ital.*, 1978, **108**, 425.
17 G. Alagona, P. Desmeules, C. Ghio, and P. A. Kollman, *J. Am. Chem. Soc.*, 1984, **106**, 3623.
18 S. J. Weiner, G. L. Seibel, and P. A. Kollman, *Proc. Natl. Acad. Sci. USA*, 1986, **83**, 649.
19 D. M. Blow, J. J. Birktoft, and B. S. Hartley, *Nature* (*London*), 1969, **221**, 337.

20 T. A. Steitz and R. G. Shulman, *Ann. Rev. Biophys. Bioeng.*, 1982, **11**, 419.
21 P. K. Weiner and P. A. Kollman, *J. Comp. Chem.*, 1981, **2**, 287.
22 Chemical Design Ltd., Oxford, U.K.
23 P. B. Hitchcock, R. Mason, K. M. Thomas, and G. G. Shipley, *Proc. Natl. Acad. Sci. USA*, 1974, **71**, 3036.
24 M. F. Guest and J. Kendrick, GAMESS User Manual, CCP1/86/1, Daresbury Laboratory, UK, 1986.
25 H. Umeyama, A. Imamura, and C. Nagata, *J. Theor. Biol.*, 1973, **41**, 485.
26 S. Scheiner, D. A. Kleier, and W. N. Lipscomb, *Proc. Natl. Acad. Sci. USA*, 1975, **72**, 2606.
27 S. Scheiner and W. N. Lipscomb, *Proc. Natl. Acad. Sci. USA*, 1976, **73**, 432.
28 S. Nakagawa and H. Umeyama, *Bioorg. Chem.*, 1982, **11**, 322.
29 H. Umeyama, S. Nakagawa, and T. Kudo, *J. Mol. Biol.*, 1981, **150**, 409.

Received 10*th March* 1989; *Paper* 9/01053J